Data-based estimates of ocean carbon uptake biased high from neglect of submonthly atmospheric pressure variability

Authors: Jeanne Dombret[1], Hugo Bellenger[1], Xavier Perrot[1], Laëtitia Parc[1], Lester Kwiatkowski[2], Frédéric Chevallier[3], Laurent Bopp[1], Marion Gehlen[3], Roland Séférian[4], Sarah Berthet[4] and James C. Orr[3]

Affiliations :

[1] Laboratoire de Météorologie Dynamique, LMD-IPSL, École Normale Supérieure, Université PSL, École polytechnique, Institut Polytechnique de Paris, Sorbonne Université, CNRS, Paris France.

[2] Laboratoire d'Océanographie et du Climat : Expérimentations et Approches Numériques, LOCEAN-IPSL, Sorbonne Université-CNRS-IRD-MNHN, Paris, France

[3] Laboratoire des Sciences du Climat et de l'Environnement, LSCE-IPSL, CEA-CNRS-UVSQ, Université Paris Saclay, Gif-sur-Yvette, France

[4] Centre National de Recherches Météorologiques (CNRM), Université de Toulouse, Météo-France, CNRS, Toulouse, France.

Correspondance : Hugo Bellenger (hugo.bellenger@lmd.ipsl.fr)

Manuscript submitted to Biogeosciences

Key points

- Neglect of submonthly variability of atmospheric pressure in data-based ocean carbon sink estimates causes a positive bias of 0.12 Pg C yr^{-1}
- This bias represents on average 25% of the gap between model and data-based estimates of the sink between 2008 and 2019

- This bias is driven by the covariance between wind speed and atmospheric pressure, 85% of which stems from the southern midlatitudes

Abstract

Current estimates of the global ocean carbon sink based on measurements of CO_2 fugacity are inconsistent with those obtained from global ocean biogeochemistry models. Here we investigate how this gap might change by more fully accounting for submonthly variability in observation-based estimates, a step closer to the roughly hourly frequencies used in models. While these data-based estimates use hourly to 6-hourly wind speeds to compute the air-sea CO_2 flux, other input variables are available only at monthly resolution. Thus, they neglect high-frequency variability in key variables such as atmospheric pressure associated with synoptic events such as storms. To evaluate this error, we compare flux estimates from observational data sets with different temporal resolutions. Accounting for hourly variations in atmospheric pressure and daily variations in sea surface temperature, a data-based approach reduces the estimated global carbon uptake by 0.12 Pg C yr^{-1}, closing 25% of the average gap between observation-based and model estimates. This reduction results from proper accounting of the covariance between wind speed and atmospheric pressure, particularly in the southern extratropics.

Plain language summary

Estimates of ocean CO_2 uptake based on atmospheric and oceanic observations typically rely on monthly averages, except for wind speed. This means they miss the effects of shorter-term events such as storms, unlike models. Here we account for the impact of this short-term variability on ocean carbon uptake and find that estimated uptake is reduced, mainly because storms lower atmospheric pressure. This refinement closes about 25% of the gap between observation-based and model-based estimates.

1. Introduction

The ocean absorbs one-fourth of anthropogenic CO_2 emissions, playing a major role in the global carbon cycle. It is estimated to have absorbed 2.9 Pg C yr^{-1} of anthropogenic carbon during 2014-2023 based on the Global Carbon Budget (GCB, Friedlingstein et al. 2025). But this average value comes with a spread of more than 1 Pg C yr^{-1} between the lowest and highest estimates. The GCB is updated annually to reflect the evolution in the data and methods used to obtain the latest estimates of global carbon emissions and carbon storage in different reservoirs (sinks). Its ocean estimate relies on two different approaches.

The first approach uses global ocean biogeochemistry models (GOBMs), each of which couples a global-scale, general ocean circulation model to an ocean carbon cycle component. GOBMs simulate ocean transport of dissolved inorganic carbon (DIC) and total alkalinity (Alk), from which is calculated surface ocean CO_2 fugacity ($fCO_{2\,sea}$), a variable nearly identical to the ocean partial pressure of CO_2 (pCO_{2sea}). From that, the models compute the difference relative to the atmospheric CO_2 fugacity ($fCO_{2\,atm}$), multiplying that difference by a gas transfer velocity times the solubility to compute the air-sea CO_2 flux. The simulated air-sea CO_2 flux is affected by multiple physical atmospheric variables since the gas transfer velocity is often parameterized as a quadratic function of wind speed and $fCO_{2\,atm}$ depends in part on atmospheric pressure and vapor pressure. GOBMs are typically forced by atmospheric reanalyses having hourly to 6-hourly timesteps. Nonetheless, simulated ocean uptake of anthropogenic carbon in GOBMs is only weakly sensitive to uncertainties in the gas transfer velocity. For example, a doubling of the gas transfer velocity led to only a 9% increase in simulated ocean uptake of anthropogenic carbon (Sarmiento et al., 1992). The extra CO_2 added to the ocean from enhanced gas exchange is not transported away from the surface quickly enough, thus increasing the simulated $fCO_{2\,sea}$ and reducing the change in the air-sea flux, a key feedback inherent not only

in models but also in the real ocean. While models have their own problems, such as biases in simulated circulation fields, they are insensitive to the magnitude of the gas transfer velocity.

The second approach uses observation-based products for fCO_{2sea} rather than modeled fields. These data products rely on millions of in situ measurements of fCO_{2sea} archived in the Surface Ocean CO_2 Atlas (SOCAT, Bakker et al., 2016). Many groups have used this unevenly spaced data to produce evenly spaced gridded data products, mapping it typically to a 1°×1° grid with monthly resolution and filling missing grid cells based on a series of global predictors, e.g., sea surface temperature and mixed-layer depth, obtained from satellite products and atmospheric and oceanic reanalyses (Landschützer et al., 2016; Rödenbeck et al., 2022; Chau et al., 2024 Watson et al., 2020; Zeng et al., 2022; Iida et al., 2021; Gregor et al., 2024; Gloege et al., 2022; Gregor et al. 2019). Using observed rather than simulated fCO_{2sea} is an advantage since it reflects the real ocean's air-sea interaction. But it comes with a disadvantage: the data-based approach cannot benefit from the previously mentioned feedback between the flux and $fCO_{2\ sea}$. Thus, compared to the GOBMs, data-based estimates of air-sea CO_2 fluxes are more sensitive to errors in the bulk flux parameterization, with associated uncertainties scaling proportionally to the imposed gas transfer velocity (Gloege et al. 2025, Jersild and Landschützer 2024).

It is estimated that the ensemble mean 1-σ uncertainty for the 10 models is 0.5 Pg C yr^{-1} while that for the 8 data products is 0.6-0.7 Pg C yr^{-1} considering both random and systematic uncertainties (Friedlingstein et al., 2025; Ford et al., 2024). Moreover, there is a systematic discrepancy between the two approaches, where the average sink from data-based products is 0.5 Pg C yr^{-1} larger than that from GOBMs. Friedlingstein et al. (2025) suggest a possible 10%-20% underestimate from the GOBMs for the ocean uptake of anthropogenic carbon owing to several potential problems: an overestimated Revelle factor, salinity biases in the Southern Ocean, an underestimated penetration of carbon into the ocean interior from weak vertical

mixing and transport, and a delayed beginning for the anthropogenic perturbation, after the actual start of the industrial era (see Bronselear et al., 2017, Terhaar et al. 2022, Terhaar et al. 2025).

Other potential sources of model-data discrepancy come from the data-based approach. First, there is the 0.65 ± 0.15 Pg C yr^{-1} that must be added to the data-based estimates to back calculate the anthropogenic carbon flux from the total flux by removing the global effect of the net preindustrial outgassing driven by the natural imbalance between riverine input and sediment loss of carbon (Aumont et al., 2001; Regnier et al., 2022), as discussed by DeVries et al. (2023), Perez et al. (2024) and Planchat et al. (2025). Another important source of uncertainty is the sparsity of SOCAT measurements in some key regions such as the Southern Ocean (Hauck et al., 2020, 2023; Ford et al., 2024). Finally, discrepancies may also stem from the very different temporal resolutions of the two approaches. While GOBMs compute air-sea CO_2 fluxes with a time step on the order of an hour, the data-based products used in GCB 2024 generally rely on monthly averaged variables. Fortunately, the data-based products do account for the effect of submonthly wind-speed variance by using monthly means of the square of observed 1- to 6-hourly wind speed when computing the gas transfer velocity. But they neglect nonlinearities stemming from submonthly variability of other physical drivers, including atmospheric pressure, sea surface temperature, and sea surface salinity.

To address this limitation, Gregor et al. (2024) developed a higher-frequency data product computing the CO_2 flux with 8-day temporal resolution, but they also showed its use had minimal effect on the resulting global sink estimate. Unfortunately, an 8-day frequency still does not resolve intense meteorological events, such as tropical cyclones and extratropical storms, which drive variations in atmospheric and oceanic variables on shorter time scales. Previous case studies have shown that tropical cyclones can cause substantial regional ocean carbon uptake (Gregor et al., 2024) or outgassing (Bates et al., 1998; Huang & Imberger, 2010),

depending largely on the initial sign of the CO_2 fugacity difference at the air-sea interface. Yet the resulting global contribution of tropical cyclones to the ocean carbon sink is negligible (Lévy et al. 2012) because they mostly occur in regions with weak air-sea differences in fCO_2 and because they increase CO_2 fluxes both into and out of the ocean, nearly canceling one another. Extratropical studies with data from floats and gliders indicate that storms in the Southern Ocean can provoke outgassing anomalies over 1-3 days, driven by concomitant variations in wind speed, atmospheric pressure, and DIC concentrations (Carranza et al., 2024; Nicholson et al., 2022). The Argo float-based estimates suggest that Southern Ocean storms may reduce the global carbon sink by up to 0.057 Pg C yr^{-1} (Carranza et al., 2024). But storms represent only a part of the submonthly phenomena. It remains uncertain how high-frequency variability, if it were properly accounted for in data-based approaches, would affect resulting estimates of the air-sea CO_2 flux at the global scale.

Although submonthly and particularly synoptic variability of ocean biogeochemical variables (fCO_2, DIC…) cannot yet be constrained at the global scale due to the scarcity of observations, such is not the case for physical variables including not only wind speed but also atmospheric pressure, sea surface temperature and salinity. Here we ask how much this submonthly variability might affect observation-based estimates of the global ocean carbon sink, particularly in mid-latitudes where storms induce outgassing through simultaneous decreases in atmospheric pressure and increases in wind speed. Our aim is to quantify the importance of this effect, identifying the responsible non-linearities between variables and the regions where they dominate.

2. Methods

2.1 CO_2 flux calculations

147 Consistent with the GCB, our data-based air-sea CO_2 flux F is computed as

148 $$F = k_{660}(u)A(T,S)(fCO_{2atm} - fCO_{2sea}). \quad (1)$$

149 where k_{660} is the gas transfer (piston) velocity at 20°C, fCO_{2atm} and fCO_{2sea} are the
150 fugacities of CO_2 in the atmosphere and the ocean, and $A = K_0(T,S)\left(\frac{Sc(T)}{660}\right)^{\frac{-1}{2}}$ with K_0 being
151 the solubility of CO_2 in seawater computed from the sea surface temperature (T) and salinity
152 (S) (Weiss, 1974), and the Schmidt number (Sc) ratio is used to adjust the wind-speed
153 formulation for gases other than CO_2 and for temperatures other than 20°C (Wanninkhof, 2014).
154 Positive fluxes indicate an air-to-sea CO_2 flux. The k_{660} is calculated using a quadratic function
155 of the 10-m wind speed $k_{660} = au^2$ (Wanninkhof, 1992), and u is the wind speed at 10 m. As
156 for a, it is an empirical scaling constant adjusted for each wind dataset so that the corresponding
157 global value of k (i.e., k_{660} normalized to different temperatures with the Schmidt number ratio
158 above) averages 16.5 cm hr^{-1} over the ice-free ocean as derived from the observed global bomb
159 ^{14}C inventory (Naegler, 2009). Since it is based on the real ocean inventory of bomb ^{14}C, this
160 scaling approach should inherently account for the effects of submonthly variability of all
161 variables that affect the gas transfer velocity; however there is a 20% uncertainty associated
162 with the bomb ^{14}C inventory and thus k.

163 The CO_2 fugacity in the atmosphere, fCO_{2atm}, is the partial pressure of CO_2 corrected for the
164 non-ideal behaviour of the gas. The fCO_{2atm}, (in μatm) is computed from the mixing ratio (or
165 mole fraction) of CO_2 (in ppm), which is measured in dried air, as follows

166 $$fCO_{2atm} = \phi_{CO_2}(P_{atm},T)X_{CO_2}\left(P_{atm} - P_{vap}(T,S)\right) \quad (2)$$

167 where ϕ_{CO_2} is the fugacity coefficient from Weiss (1974), X_{CO_2} is the CO_2 mole fraction in dry
168 air (ppm), P_{atm} is the surface atmospheric pressure (atm), and P_{vap} is the partial pressure of

169 water vapor (atm) from Weiss & Price (1980), an empirical function of T and S assuming that
170 the air is fully saturated (100% humidity) just above the air-sea interface.

171 For simplicity, in contrast with GCB data-based product, our oceanic fugacity fCO_{2sea}
172 is not from an ocean fCO_2 observation product but is instead computed from gridded products
173 of T, S, DIC, Alk, and total inorganic phosphorus and silicon concentrations ($[P]$ and $[Si]$) using
174 mocsy (Orr & Epitalon, 2015). This simplification enables us to evaluate the impact of
175 submonthly variability of T and S on fCO_{2sea} while maintaining the basic GCB data-based
176 approach.

177 We use hourly fields of wind speed u and surface pressure P_{atm}, and daily fields of sea
178 surface temperature T and sea ice concentration from the fifth generation ECMWF reanalysis
179 (ERA5, Hersbach et al., 2020) at 0.25°×0.25° spatial resolution. In the gas transfer velocity
180 formulation, the empirical scaling constant a is taken to be 0.271 as computed for the ERA5
181 wind speed field by Fay et al. (2021). We also use the bulk daily sea surface temperature rather
182 than the hourly sea-surface skin temperature to be consistent with current GCB data-based
183 estimates. All but one of those estimates use bulk sea surface temperature. Thus, we do not
184 include effects of diurnal warming and cool skin that have been addressed in previous studies
185 (Watson et al. 2020, Dong et al. 2022, Bellenger et al. 2023). Sea-surface salinity S is taken
186 from the Multi Observation Global Ocean Sea Surface Salinity and Sea Surface Density dataset
187 (Droghei et al., 2018) with 0.25°×0.25° spatial resolution and 8-day temporal resolution.
188 Atmospheric CO_2 dry air mole fraction X_{CO2} is from the NOAA Greenhouse Gas Marine
189 Boundary Layer Reference (Lan et al., 2023), provided as 4.5° latitudinal bands at a temporal
190 resolution of ~8 days. For X_{CO2}, we computed its monthly means because of the limited
191 observational network used to produce this global data set, thus leaving the impact of its
192 submonthly variability for future studies. Fields of DIC and Alk are from OceanSODA-ETHZ
193 (Gregor & Gruber, 2021), which has 1°×1° spatial resolution and monthly temporal resolution.

Fields of $[P]$ and $[Si]$ are from a monthly climatology (Broullón et al., 2019) derived from the 2013 World Ocean Atlas dataset (Boyer et al., 2013), also on a 1°×1° grid. Before computing fluxes, all datasets are regridded to a common 0.25°×0.25° grid using bilinear interpolation. Air-sea CO_2 fluxes are calculated from 2009 to 2018 and, for simplicity, only for latitudes between 60°S and 60°N, thus avoiding most sea-ice covered areas. Calculations consider only the time steps when grid cells have no ice cover. Regions poleward of 60° contribute only marginally to the global sink (Takahashi et al., 2009). Table 1 summarizes the data used in this study.

To study the sensitivity of the global ocean carbon sink to the submonthly variability that is neglected in GCB data-based products, we computed two estimates: (1) our reference, using monthly averages for all variables except for wind speed, which as in GCB already accounts for submonthly wind speed variance; and (2) our test case, using instead higher temporal resolution data for atmospheric pressure, sea-surface temperature, and sea surface salinity. Consistent with the temporal resolution of GCB 2024 data products, the reference flux F_{ref} is calculated using the monthly mean of the squared wind speed computed from hourly data $\overline{u^2}$ and monthly means of the other variables:

$$F_{ref} = a\overline{u^2}A\left(\overline{T},\overline{S}\right)\Delta fCO_2\left(\overline{P_{atm}},\overline{T},\overline{S},\overline{X_{CO2}},\overline{DIC},\overline{Alk},\overline{[P]}^c,\overline{[Si]}^c\right) \quad (3)$$

The overbar denotes a monthly mean, while the appended c superscript indicates a climatological monthly mean. The high-frequency flux F_h is calculated hourly using each variable at its highest available temporal resolution (hourly u and P_{atm}, daily T, 8-daily S, and monthly for all others). We compare F_{ref} to $\overline{F_h}$, the monthly mean of F_h :

$$\overline{F_h} = \overline{au^2A(T,S)\Delta fCO_2\left(P_{atm},T,S,\overline{X_{CO2}},\overline{DIC},\overline{Alk},\overline{[P]}^c,\overline{[Si]}^c\right)} \quad (4)$$

To further assess the causes of differences, we also compare F_{ref} and $\overline{F_h}$ to the monthly averages of two intermediate air-sea CO_2 fluxes: (1) $\overline{F_P}$ which is computed like $\overline{F_h}$ but using hourly P and monthly T and S and (2) $\overline{F_{P,T}}$, which is computed using hourly P_{atm}, daily T, and monthly S. Then the difference $\overline{F_P} - F_{ref}$ shows the importance of taking into account high-frequency variability of P_{atm}, Another difference $\overline{F_{P,T}} - \overline{F_P}$ reflects the importance of taking into account daily T, while $\overline{F_h} - \overline{F_{P,T}}$ shows the impact of submonthly variations of S.

Finally, the corresponding global ocean sinks of anthropogenic carbon S_h and S_{ref} are obtained by spatially integrating the air-sea CO_2 flux (between 60°S and 60°N), and correcting for preindustrial outgassing by subtracting the global $S_{river} = 0.65 \pm 0.15 PgCyr^{-1}$ (Regnier et al., 2022).

We consider that the differences $\overline{F_h} - F_{ref}$ and $S_h - S_{ref}$ are statistically significant only if they differ from 0 at the 99% level using Student's t-test.

2.2 Reynolds decomposition

To investigate the non-linearities between high-frequency variations of the variables that are responsible for differences between F_{ref} and $\overline{F_h}$, a Reynolds decomposition is used with respect to u and $\Delta = fCO_{2atm} - fCO_{2sea}$ for each month from 2009 to 2018, assuming that the solubility and Schmidt number variations cancel out to give $A = \overline{A}$ (Etcheto et Merlivat 1988), an assumption good to within 5% locally (Wanninkhof, 2014):

$$F_h = aA\overline{u}^2\overline{\Delta} + aA(u')^2\overline{\Delta} + 2aA\overline{u}u'\Delta' + aA(u')^2\Delta' + aA\overline{u}^2\Delta' + 2aA\overline{u}u' \quad (5)$$

whose monthly mean is

$$\overline{F_h} = \underbrace{\underbrace{aA\overline{u}^2\overline{\Delta}}_{meanbulk} + \underbrace{aA\overline{(u')^2\Delta}}_{variance}}_{bulkterm} + \underbrace{\underbrace{2aA\overline{u}\overline{u'\Delta'}}_{covariance} + \underbrace{aA\overline{(u')^2\Delta'}}_{3rdordermoment}}_{correctionterms} \quad (6)$$

The combination of the first term (mean bulk) and 2nd term (variance) is referred to as the bulk term $\left(aA\overline{u^2}\overline{\Delta} = aA\overline{u}^2\overline{\Delta} + aA\overline{(u')^2}\overline{\Delta}\right)$. Thus by definition it includes the enhancement from wind speed variance. The bulk term is very close to the reference flux F_{ref}. This agreement along with the assumption that $A = \overline{A}$ is illustrated by the mean difference between F_{ref} and the bulk term $\left(aA\overline{u^2}\overline{\Delta}\right)$, which ranges from 0 to - 0.2 g C m^{-2} yr^{-1} (Figure S1), an order of magnitude smaller than the mean differences between $\overline{F_h}$ and F_{ref} (Figure 1c). This bulk term (mean bulk and variance in (6)) is the same as the GCB flux definition. GCB and other data-based reconstructions do not take into account the final two terms of equation (6), the correction terms. The first of those (u and Δ covariance term) accounts for how the flux is affected by covariation between wind speed anomalies and Δ anomalies (2nd-order moment). The second of the correction terms (3rd-order mixed moment) accounts for nonlinear interactions between wind speed variance and Δ anomalies, thus capturing effects from skewness or asymmetry in fluctuations.

3. Results

3.1 Global ocean carbon sink sensitivity to submonthly variability

Our estimate S_{ref} is comparable in magnitude to the average from the GCB data products although it does not capture the precise interannual evolution, in particular after 2016 (Figure 1a). This difference stems from the latest version of the DIC and Alk OceanSODA-ETHZ dataset (v2021, Gregor et al. 2021), which does not capture the change in Alk, DIC and fCO_{2sea} associated with the slowdown in ocean sink after 2016 (e.g. Friedlingstein et al. 2022). This slowdown indeed only emerged in GCB data-based products after GCB 2023 (e.g. Friedlingstein et al. 2025). Both our S_{ref} and GCB account for submonthly variability of u. Our sink estimate S_h also accounts for submonthly variability of P_{atm}, T, and S, and it is 0.12 Pg C yr^{-1} lower than S_{ref}. Therefore, the standard approach, which neglects all submonthly

variability besides that of u, overestimates the carbon sink by 0.12 P g C yr^{-1}. On average between 2009 and 2018, this difference corresponds to 5% of the carbon sink S_{ref} but 25% of the discrepancy between models and data products from GCB (~0.5 Pg C yr^{-1}). Our computed difference does not change over 2009 to 2018 and remains statistically significant.

The spatial distribution of F_{ref} (Fig. 1b) is consistent with the fluxes from the SeaFlux product (Fay et al. 2021, Figure S2). The 2009-2018 mean difference $\overline{F_h} - F_{ref}$ shows that the discrepancy between the two fluxes stems largely from latitudes between 30° and 60° in both hemispheres (Figure 1c). In these regions relative to F_{ref}, $\overline{F_h}$ exhibits either more outgassing (North Atlantic, Southern Ocean) or less uptake (North Pacific, by 1.5 g C m^{-2} yr^{-1} on average). A weaker opposing effect is seen in tropics, where sinks are increased by 0.5 g C m^{-2} yr^{-1} on average, and by up to 1 g C m^{-2} yr^{-1} in the Arabian Sea and South China Sea.

Differences in the mid-latitudes are mainly due to atmospheric pressure variations, whereas differences in the tropics are driven by sea surface temperature variations. The former can be seen in the $\overline{F_P} - F_{ref}$ map (Figure 2a) and the $\overline{F_{P,T}} - \overline{F_P}$ map (Figure 2b). Atmospheric pressure variations reduce the carbon sink estimate by 0.136 Pg C yr^{-1} on average, an effect that is slightly weakened by sea surface temperature variations which increase the sink by 0.016 Pg C yr^{-1}. On synoptic timescales (2-10 days), low pressure perturbations are associated with stronger winds, so periods of strong CO_2 exchange have lower atmospheric pressure and thus lower atmospheric CO_2 fugacity. Thus wind speed and atmospheric pressure covariance leads to an anomalous outgassing correction term in the midlatitudes. Further separation of $\overline{F_{P,T}} - \overline{F_P}$ into atmospheric and oceanic components (Figure S3b) reveal that temperature variations mainly affect ocean fCO_{2sea}, but have negligible effect on vapor pressure. The anomalous ingassing in the Arabian Sea appears to result from an increase in submonthly variability of

wind speed, which drives stronger upwelling and hence surface cooling, thus reducing fCO_{2sea}. The remaining effect of salinity ($\overline{F_h} - \overline{F_{P,T}}$) is negligible.

3.2 Relative importance of the correction terms

The Reynolds decomposition (5) reveals the relative importance of the different terms in equation (5). The wind speed variance term, which is already accounted for in the GCB data-based products, is the dominant source of submonthly nonlinearity (Fig 3a). It results in an increase in the estimated 60°N-60°S ocean carbon sink by 0.36 Pg C yr^{-1}. This increase is situated mainly in the mid-latitudes, peaking at 40°S and 40°N (Fig. 3, S4).

Our first correction term (covariance) accounts for 90% of the correction, whereas the third-order moment is weaker. Together they result in a global outgassing anomaly whose magnitude is one-third of the wind variance term and opposite in sign. About 85% of this contribution is situated between 60°-30°S and amounts to a reduction of 0.1 Pg C yr^{-1} (Fig. 3a). The other main region where the correction terms reduce the sink is between 30°-60°N, but that reduction of 0.03 Pg C yr^{-1} is largely offset by the 0.026 Pg C yr^{-1} increase between 30°S-30°N. Although the covariance term is generally weaker than the wind speed variance term, it has a similar magnitude in the tropics and dominates south of 50°S (Figure 3b).

4. Discussion

This study reveals that accounting for hourly variability in atmospheric pressure and including the small compensation from daily variability in sea surface temperature, reduces data-based estimates of the global ocean carbon sink by 0.12 Pg C yr-1, thereby closing 25% of the gap between those data products and the GOBMs. While the 8-day product from Gregor et al. (2024) offers higher frequency atmospheric and oceanic CO_2 fugacities than the standard

monthly products used in the GCB data-based ocean flux estimates, the resulting computed global flux is essentially unchanged. Thus, it appears that at least synoptic frequency is needed to adequately capture the effect of atmospheric variability. Whether or not 6-hourly or daily atmospheric pressure data would be sufficient in place of our use of hourly data remains a question for future research.

The Reynolds decomposition of the high-resolution CO_2 flux confirms that the submonthly variation in wind speed, already accounted for in the ocean data products, is the most important nonlinearity. It generally increases sink estimates outside the tropics with peaks at 40°S and 40°N. Conversely, our correction due to the submonthly covariance of wind speed and atmospheric pressure leads to outgassing anomalies in the midlatitudes. The reason is that midlatitude synoptic disturbances have strong winds that favor air-sea exchange but also reduce atmospheric pressure, thus lowering atmospheric CO_2 fugacity, which favors outgassing. This correction is particularly large in waters south of 30°S, representing 85% of its impact on the global ocean carbon sink. South of 50°S, it becomes the main source of nonlinearity.

While the nonlinearities underlined here appear to explain 25% of the average gap between models and data-based products, their effect seems constant in time. Therefore, they do not seem to explain the temporal evolution of the gap underlined by Friedlingstein et al. (2025). The exact correction will depend on the calculation details and thus will differ between data-based products. For future GCB exercises, we suggest that each group compute independently both directions of the flux $k_{660}(u)A(T,S)fCO_{2atm}$ and $k_{660}(u)A(T,S)fCO_{2sea}$ at maximum temporal resolution before computing monthly averages and taking the difference to obtain the flux. We also leave for future studies the question of whether or not accounting for submonthly variations in atmospheric X_{CO2}, particularly those due to covariations with P_{atm}, may substantially alter data-based estimates of ocean carbon uptake. The gap between data-based products and GOBMs also depends on model resolution and their representation of coastal

regions (e.g. Resplandy et al. 2024) as well as on processes not yet commonly included in the flux parameterization, such as the ocean cool skin (+0.3 Pg C yr-1, Dong et al. 2022), rain (+0.14-0.19 Pg C yr-1, Parc et al. 2024) and wave breaking-induced bubbles. While these bubbles may increase modeled CO_2 uptake by only 0.07 Pg C yr-1 (Rustogi et al., 2025), they could increase data-based estimates by up to 0.3-0.4 Pg C yr^{-1} (Dong et al., 2025). Similarly, Bellenger et al. (2023) showed that the cool skin temperature effect is three times smaller in a model framework because of the feedback process mentioned earlier and because gas exchange is not rate limiting, unlike carbon transfer to the ocean interior. Including the cool skin effect in both data-based products and GOBMs could thus increase the gap by about +0.2 Pg C yr-1. The addition of new processes in the calculation of carbon fluxes may further increase the gap between estimates from data-based products versus GOBMs.

Our results suggest that the previous estimate of the storm-induced outgassing for the Southern Ocean of 0.057 Pg C yr^{-1} (Carranza et al., 2024) is only a fraction of the total effect of submonthly variability on the ocean sink in this region. Indeed, we found a mean outgassing of about 0.1 Pg C yr^{-1} in the 60°-30°S band mainly driven by atmospheric pressure and wind speed covariance. On the other hand, previous observations in the Southern Ocean from Argo floats (Carranza et al., 2024) and gliders (Nicholson et al., 2022) suggest that submonthly variability of ocean biogeochemical variables have a major impact on storm induced outgassing. Those observations suggest that entrainment of cold, DIC-rich subsurface water into the surface mixed layer is the leading cause of mean storm-driven CO_2 outgassing in the Southern Ocean (Carranza et al., 2024). Monthly fCO_2-products cannot resolve storm induced fCO_{2sea}, while GOBMs may underestimate storm-driven vertical transport of DIC (Carranza et al. 2024). Therefore, submonthly variability of biogeochemical variables in the Southern Ocean demands more attention, both for data- and model-based estimates. While our study helps to narrow the data-model gap, its continued growth and the large disparities among data-based products and

among models underscore the need for further advances to constrain ocean carbon uptake, advances that are also key to reducing, by difference, much larger uncertainties associated with the terrestrial biosphere.

Author contributions: Conceptualization JD, HB, XP, JCO; Methodology: LP, XP, JCO, Formal analysis: JD, XP, HB; Visualization: JD; Writing: JD, HB, JCO, LK, FC, LB, MG, RS, SB.

Acknowledgments

This study has been conducted using EU Copernicus Marine Service Information; https://doi.org/10.48670/moi-00051. To process the data, this study benefited from the IPSL mesocenter ESPRI facility which is supported by CNRS, UPMC, Labex L-IPSL, CNES and Ecole Polytechnique. JCO and MG were funded by EU grant 101083922 (OceanICU). RS acknowledges funding from the EU's Horizon Europe research and innovation programme under ESM2025 (grant agreement No 101003536) and OptimESM (grant agreement No 101081193) as well as the ANR - France 2030 as part of the PEPR TRACCS programme under grant number ANR-22-EXTR-0009.

Data availability

Estimates of the CO_2 fluxes for the different diagnostics made here are publicly available at the Zenodo repository https://doi.org/10.5281/zenodo.15848192. ERA5 reanalysis data from the ECMWF (Hersbach, H. et al., 2020) was obtained through the Copernicus Climate Change Service (C3S, 2023) (https://cds.climate.copernicus.eu/cdsapp#!/dataset/reanalysis-era5-single-levels). The results contain modified Copernicus Climate Change Service information 2020. Neither the European Commission nor ECMWF is responsible for any use that may be made of the Copernicus information or data it contains. The CO_2 dry air mole fraction data are from the NOAA Greenhouse Gas Marine Boundary Layer Reference

(https://gml.noaa.gov/ccgg/mbl/data.php). The sea surface salinity values were downloaded from EU Copernicus Marine Service Information (https://doi.org/10.48670/moi-00051). Global DIC and Alk bulk values are from the OceanSODA–ETHZ climatology dataset (https://www.ncei.noaa.gov/access/metadata/landing-page/bin/iso?id=gov.noaa.nodc:0220059). The Broullón et al. (2020) monthly climatologies of dissolved inorganic silicon and phosphorus are available at https://digital.csic.es/handle/10261/184460.

References

Aumont, O., Orr, J. C., Monfray, P., Ludwig, W., Amiotte-Suchet, P., and Probst, J.-L., 2001: Riverine-driven interhemispheric transport of carbon, Global Biogeochem. Cy., 15, 393–405, https://doi.org/10.1029/1999GB001238

Bakker, D. C. E., Pfeil, B., Landa, C. S., Metzl, N., O'Brien, K. M., Olsen, A., Smith, K., Cosca, C., Harasawa, S., Jones, S. D., Nakaoka, S., Nojiri, Y., Schuster, U., Steinhoff, T., Sweeney, C., Takahashi, T., Tilbrook, B., Wada, C., Wanninkhof, R., … Xu, S. (2016). A multi-decade record of high-quality fCO2 data in version 3 of the Surface Ocean CO2 Atlas (SOCAT). Earth System Science Data, 8(2), 383–413. https://doi.org/10.5194/essd-8-383-2016

Bates, N. R., Knap, A. H., & Michaels, A. F. (1998). Contribution of hurricanes to local and global estimates of air–sea exchange of CO2. *Nature*, *395*(6697), 58–61. https://doi.org/10.1038/25703

Bellenger, H., Bopp, L., Ethé, C., Ho, D., Duvel, J. P., Flavoni, S., Guez L., T. Kataoka, X. Perrot, L. Parc, and M. Watanabe (2023). Sensitivity of the global ocean carbon sink to the ocean skin in a climate model. Journal of Geophysical Research : Oceans, 128, e2022JC019479. https://doi.org/10.1029/2022JC019479

Boyer, T.P., Antonov, J.I., Baranova, O.K., Coleman, C., Garcia, H.E., Grodsky, A., Johnson, D.R. Locarnini, R.A., Mishonov, A.V., O'Brien,T.D., Paver, C.R., Reagan,J.R., Seidov, D., Smolyar, I.V. and Zweng, M.M. (2013) World Ocean Database 2013. Silver Spring, MD, National Oceanographic Data Center, 208pp. (NOAA Atlas NESDIS, 72). DOI: https://doi.org/10.25607/OBP-1454

Bronselaer, B., Winton, M., Russell, J., Sabine, C. L., & Khatiwala, S. (2017). Agreement of CMIP5 simulated and observed ocean anthropogenic CO2 uptake. Geophysical Research Letters, 44, 12,298–12,305. https://doi.org/10.1002/2017GL074435

Broullón, D., Pérez, F. F., Velo, A., Hoppema, M., Olsen, A., Takahashi, T., Key, R. M., Tanhua, T., González-Dávila, M., Jeansson, E., Kozyr, A., & van Heuven, S. M. A. C. (2019). A global monthly climatology of total alkalinity: A neural network approach. *Earth System Science Data*, *11*(3), 1109–1127. https://doi.org/10.5194/essd-11-1109-2019

Carranza, M. M., Long, M. C., Di Luca, A., Fassbender, A. J., Johnson, K. S., Takeshita, Y., Mongwe, P., & Turner, K. E. (2024). Extratropical storms induce carbon outgassing over the Southern Ocean. *Npj Climate and Atmospheric Science*, *7*(1), 1–16. https://doi.org/10.1038/s41612-024-00657-7

Chau, T.-T.-T., Chevallier, F., & Gehlen, M. (2024). Global analysis of surface ocean CO2 fugacity and air-sea fluxes with low latency. Geophysical Research Letters, 51, e2023GL106670. https://doi.org/10.1029/2023GL106670

DeVries, T., Yamamoto, K., Wanninkhof, R., Gruber, N., Hauck, J., Müller, J. D., et al. (2023). Magnitude, trends, and variability of the global ocean carbon sink from 1985 to 2018. Global Biogeochemical Cycles, 37, e2023GB007780. https://doi.org/10.1029/2023GB007780

Dong, Y., Bakker, D. C. E., Bell, T. G., Huang, B., Landschützer, P., Liss, P. S., & Yang, M. (2022). Update on the temperature corrections of global air-sea CO2 flux estimates. *Global Biogeochemical Cycles, 36*, e2022GB007360. https://doi.org/10.1029/2022GB007360

Dong, Y., Yang, M., Bell, T. G., Marandino, C. A., & Woolf, D. K. (2025). Asymmetric bubble-mediated gas transfer enhances global ocean CO2 uptake. *Nature Communications*, *16*(1), 10595. https://doi.org/10.1038/s41467-025-66652-5

Droghei, R., Buongiorno Nardelli, B., & Santoleri, R. (2018). A New Global Sea Surface Salinity and Density Dataset From Multivariate Observations (1993–2016). *Frontiers in Marine Science*, *5*. https://doi.org/10.3389/fmars.2018.00084

Etcheto, J., et L. Merlivat. 1988. « Satellite Determination of the Carbon Dioxide Exchange Coefficient at the Ocean-Atmosphere Interface: A First Step ». Journal of Geophysical Research: Oceans 93 (C12): 15669-78. https://doi.org/10.1029/JC093iC12p15669.

Fay, A. R., Gregor, L., Landschützer, P., McKinley, G. A., Gruber, N., Gehlen, M., Iida, Y., Laruelle, G. G., Rödenbeck, C., Roobaert, A., & Zeng, J. (2021). SeaFlux: Harmonization of air–sea CO_2 fluxes from surface pCO_2 data products using a standardized approach. *Earth System Science Data*, *13*(10), 4693–4710. https://doi.org/10.5194/essd-13-4693-2021

Ford, D. J., J. Blannin, J. Watts, A. J. Watson, P. Landschützer, A. Jersild, and J. D. Shutler, 2024: A comprehensive analysis of air-sea CO2 flux uncertainties constructed from surface ocean data products, Glob. Biogeochem. Cycles, 38, e2024GB008188. https://doi.org/10.1029/2024GB008188

Friedlingstein, P., Jones, M. W., O'Sullivan, M., Andrew, R. M., Bakker, D. C. E., Hauck, J., Le Quéré, C., Peters, G. P., Peters, W., Pongratz, J., Sitch, S., Canadell, J. G., Ciais, P.,

Jackson, R. B., Alin, S. R., …. Zeng, J.(2022): Global Carbon Budget 2021, Earth Syst. Sci. Data, 14, 1917–2005, https://doi.org/10.5194/essd-14-1917-2022.

Friedlingstein, P., O'Sullivan, M., Jones, M. W., Andrew, R. M., Hauck, J., Landschützer, P., Le Quéré, C., Li, H., Luijkx, I. T., Olsen, A., Peters, G. P., Peters, W., Pongratz, J., Schwingshackl, C., Sitch, S., Canadell, J. G., Ciais, P., Jackson, R. B., Alin, S. R., … Zeng, J. (2025a). Global Carbon Budget 2024. Earth System Science Data, 17(3), 965–1039. https://doi.org/10.5194/essd-17-965-2025

Gloege, L., Yan, M., Zheng, T., & McKinley, G. A. (2022). Improved Quantification of Ocean Carbon Uptake by Using Machine Learning to Merge Global Models and pCO2 Data. *Journal of Advances in Modeling Earth Systems, 14*(2), e2021MS002620. https://doi.org/10.1029/2021MS002620

Gloege, L., and Eisaman, M. D. (2025). Regional uncertainty analysis in the air–sea CO2 flux. Earth and Space Science, 12, e2024EA004032. https://doi.org/10.1029/2024EA004032

Gregor, L., Lebehot, A. D., Kok, S., & Scheel Monteiro, P. M. (2019). A comparative assessment of the uncertainties of global surface ocean CO2 estimates using a machine-learning ensemble (CSIR-ML6 version 2019a) – have we hit the wall? *Geoscientific Model Development, 12*(12), 5113–5136. https://doi.org/10.5194/gmd-12-5113-2019

Gregor, L., & Gruber, N. (2021). OceanSODA-ETHZ: A global gridded data set of the surface ocean carbonate system for seasonal to decadal studies of ocean acidification. *Earth System Science Data*, *13*(2), 777–808. https://doi.org/10.5194/essd-13-777-2021

Gregor, L., Shutler, J., & Gruber, N. (2024). High-Resolution Variability of the Ocean Carbon Sink. *Global Biogeochemical Cycles*, *38*(8), e2024GB008127. https://doi.org/10.1029/2024GB008127

Hauck, J., Zeising, M., Le Quéré, C., Gruber, N., Bakker, D. C. E., Bopp, L., Chau, T. T. T., Gürses, Ö., Ilyina, T., Landschützer, P., Lenton, A., Resplandy, L., Rödenbeck, C.,

Schwinger, J., & Séférian, R. (2020). Consistency and Challenges in the Ocean Carbon Sink Estimate for the Global Carbon Budget. *Frontiers in Marine Science*, *7*. https://doi.org/10.3389/fmars.2020.571720

Hauck, J., Nissen, C., Landschützer, P., Rödenbeck, C., Bushinsky, S., & Olsen, A. (2023). Sparse observations induce large biases in estimates of the global ocean CO 2 sink: an ocean model subsampling experiment. *Philosophical Transactions of the Royal Society A: Mathematical, Physical and Engineering Sciences, 381*(2249). https://doi.org/10.1098/rsta.2022.0063

Hersbach, H., Bell, B., Berrisford, P., Hirahara, S., Horányi, A., Muñoz-Sabater, J., Nicolas, J., Peubey, C., Radu, R., Schepers, D., Simmons, A., Soci, C., Abdalla, S., Abellan, X., Balsamo, G., Bechtold, P., Biavati, G., Bidlot, J., Bonavita, M., … Thépaut, J.-N. (2020). The ERA5 global reanalysis. *Quarterly Journal of the Royal Meteorological Society*, *146*(730), 1999–2049. https://doi.org/10.1002/qj.3803

Huang, P., & Imberger, J. (2010). Variation of pCO2 in ocean surface water in response to the passage of a hurricane. *Journal of Geophysical Research - Oceans*, *115*(C10024), Article number C10024, 11pp. https://doi.org/10.1029/2010JC006185

Iida, Y., Takatani, Y., Kojima, A., & Ishii, M. (2021). Global trends of ocean CO2 sink and ocean acidification: An observation-based reconstruction of surface ocean inorganic carbon variables. Journal of Oceanography, 77, 323–358. https://doi.org/10.1007/s10872-020-00571-5

Jersild, A., and Landschützer, P. (2024). A spatially explicit uncertainty analysis of the air-sea CO_2 flux from observations. Geophysical Research Letters,51, e2023GL106636.https://doi.org/10.1029/2023GL106636

Lan, X., Tans, P., Thoning, K., NOAA Global Monitoring, & Laboratory. (2023). MBL Reference—*NOAA Global Monitoring Laboratory* [Dataset]. https://doi.org/10.15138/DVNP-F961

Landschützer, P., Gruber, N., & Bakker, D. C. E. (2016). Decadal variations and trends of the global ocean carbon sink. *Global Biogeochemical Cycles, 30*(10), 1396–1417. https://doi.org/10.1002/2015GB005359

Lévy, M., Lengaigne, M., Bopp, L., Vincent, E. M., Madec, G., Ethé, C., Kumar, D., & Sarma, V. V. S. S. (2012). Contribution of tropical cyclones to the air-sea CO2 flux: A global view. *Global Biogeochemical Cycles*, *26*(2). https://doi.org/10.1029/2011GB004145

Naegler, T. (2009). Reconciliation of excess14C-constrained global CO2 piston velocity estimates. *Tellus B: Chemical and Physical Meteorology*, 61(2), 372. https://doi.org/10.1111/j.1600-0889.2008.00408.x

Nicholson, S.-A., Whitt, D. B., Fer, I., du Plessis, M. D., Lebéhot, A. D., Swart, S., Sutton, A. J., & Monteiro, P. M. S. (2022). Storms drive outgassing of CO2 in the subpolar Southern Ocean. *Nature Communications*, *13*(1), 158. https://doi.org/10.1038/s41467-021-27780-w

Orr, J. C., & Epitalon, J.-M. (2015). Improved routines to model the ocean carbonate system: mocsy 2.0. *Geoscientific Model Development*, *8*(3), 485–499. https://doi.org/10.5194/gmd-8-485-2015

Parc, L., Bellenger, H., Bopp, L., Perrot, X., & Ho, D. T. (2024). Global ocean carbon uptake enhanced by rainfall. Nature Geoscience, 17(9), 851–857. https://doi.org/10.1038/s41561-024-01517-y

Pérez, F. F., Becker, M., Goris, N., Gehlen, M., López-Mozos, M., Tjiputra, J., et al. (2024). An assessment of CO2 storage and sea-air fluxes for the Atlantic Ocean and

Mediterranean Sea between 1985 and 2018. Global Biogeochemical Cycles, 38, e2023GB007862. https://doi.org/10.1029/2023GB007862

Planchat, A., Bopp, L., & Kwiatkowski, L. (2025). A fresh look at the pre-industrial air-sea carbon flux using the alkalinity budget. *EGUsphere*, 1–50. https://doi.org/10.5194/egusphere-2025-523

Regnier, P., Resplandy, L., Najjar, R. G., & Ciais, P. (2022). The land-to-ocean loops of the global carbon cycle. *Nature*, *603*(7901), 401–410. https://doi.org/10.1038/s41586-021-04339-9

Resplandy, L., A. Hogikyan, J. D. Müller, R. G. Najjar, H. W. Bange, D. Bianchi, T. Weber, et al. 2024. « A Synthesis of Global Coastal Ocean Greenhouse Gas Fluxes ». *Global Biogeochemical Cycles* 38 (1): e2023GB007803. https://doi.org/10.1029/2023GB007803

Rödenbeck, C., DeVries, T., Hauck, J., Le Quéré, C., & Keeling, R. F. (2022). Data-based estimates of interannual sea–air CO2 flux variations 1957–2020 and their relation to environmental drivers. *Biogeosciences, 19*(10), 2627–2652. https://doi.org/10.5194/bg-19-2627-2022

Rustogi, P., Resplandy, L., Liao, E., Reichl, B. G., & Deike, L. (2025). Influence of wave-induced variability on ocean carbon uptake. *Global Biogeochemical Cycles*, 39, e2024GB008382. https://doi.org/10.1029/2024GB008382

Takahashi, T., Sutherland, S. C., Wanninkhof, R., Sweeney, C., Feely, R. A., Chipman, D. W., Hales, B., Friederich, G., Chavez, F., Sabine, C., Watson, A., Bakker, D. C. E., Schuster, U., Metzl, N., Yoshikawa-Inoue, H., Ishii, M., Midorikawa, T., Nojiri, Y., Körtzinger, A., … de Baar, H. J. W. (2009). Climatological mean and decadal change in surface ocean pCO2, and net sea–air CO2 flux over the global oceans. *Deep Sea Research Part*

II: Topical Studies in Oceanography, Surface Ocean CO2 Variability and Vulnerabilities, *56*(8), 554–577. https://doi.org/10.1016/j.dsr2.2008.12.009

Terhaar, J., Frölicher, T. L., and Joos, F. 2022: Observation-constrained estimates of the global ocean carbon sink from Earth system models, Biogeosciences, 19, 4431–4457, https://doi.org/10.5194/bg-19-4431-2022.

Terhaar, J., Goris, N., Müller, J. D., DeVries, T., Gruber, N., Hauck, J., et al. (2024). Assessment of global ocean biogeochemistry models for ocean carbon sink estimates in RECCAP2 and recommendations for future studies. Journal of Advances in Modeling Earth Systems, 16, e2023MS003840. https://doi.org/10.1029/2023MS003840

Wanninkhof, R. (1992). Relationship between wind speed and gas exchange over the ocean. *Journal of Geophysical Research: Oceans*, *97*(C5), 7373–7382. https://doi.org/10.1029/92JC00188

Wanninkhof, R. (2014). Relationship between wind speed and gas exchange over the ocean revisited. *Limnology and Oceanography: Methods*, *12*(6), 351–362. https://doi.org/10.4319/lom.2014.12.351

Watson, A. J., Schuster, U., Shutler, J. D., Holding, T., Ashton, I. G. C., Landschützer, P., Woolf, D. K., & Goddijn-Murphy, L. (2020). Revised estimates of ocean-atmosphere CO2 flux are consistent with ocean carbon inventory. *Nature Communications*, *11*(1), 4422. https://doi.org/10.1038/s41467-020-18203-3

Weiss, R. F. (1974). Carbon dioxide in water and seawater: The solubility of a non-ideal gas. *Marine Chemistry*, *2*(3), 203–215. https://doi.org/10.1016/0304-4203(74)90015-2

Weiss, R. F., & Price, B. A. (1980). Nitrous oxide solubility in water and seawater. *Marine Chemistry*, *8*(4), 347–359. https://doi.org/10.1016/0304-4203(80)90024-9

Wu, C., Wang, Q., Zhao, Z., & Zhang, K. (2025). Extreme CO2 Release and Its Mechanism in the Subarctic North Pacific During the Winters of 1999–2001. *Journal of Geophysical Research: Oceans*, *130*(4), e2024JC021708. https://doi.org/10.1029/2024JC021708

Zeng, J., Iida, Y., Matsunaga, T., & Shirai, T. (2022). Surface ocean CO2 concentration and air-sea flux estimate by machine learning with modelled variable trends. *Frontiers in Marine Science*, 9. https://doi.org/10.3389/fmars.2022.989233

583 **Tables**

584 **Table 1. Sources of all datasets used in this study.**

Variable	Description	Time resolution	Source
P_{atm}	Surface pressure	Hourly	ERA5
u	5m wind speed	Hourly	ERA5
Sea ice	Sea ice fraction	Hourly	ERA5
T	Sea surface temperature	Daily	ERA5
S	Sea surface salinity	8-days	Droghei et al. (2018)
DIC	Dissolved inorganic carbon	Monthly	OceanSODA-ETHZ
Alk	Alkalinity	Monthly	OceanSODA-ETHZ
X_{CO2}	CO_2 dry air mole fraction	Monthly	NOAA MBL
$[P]$	Phosphate concentration	Monthly climatology	Broullón et al. (2019)
$[Si]$	Silicate concentration	Monthly climatology	Broullón et al. (2019)

585

Figures

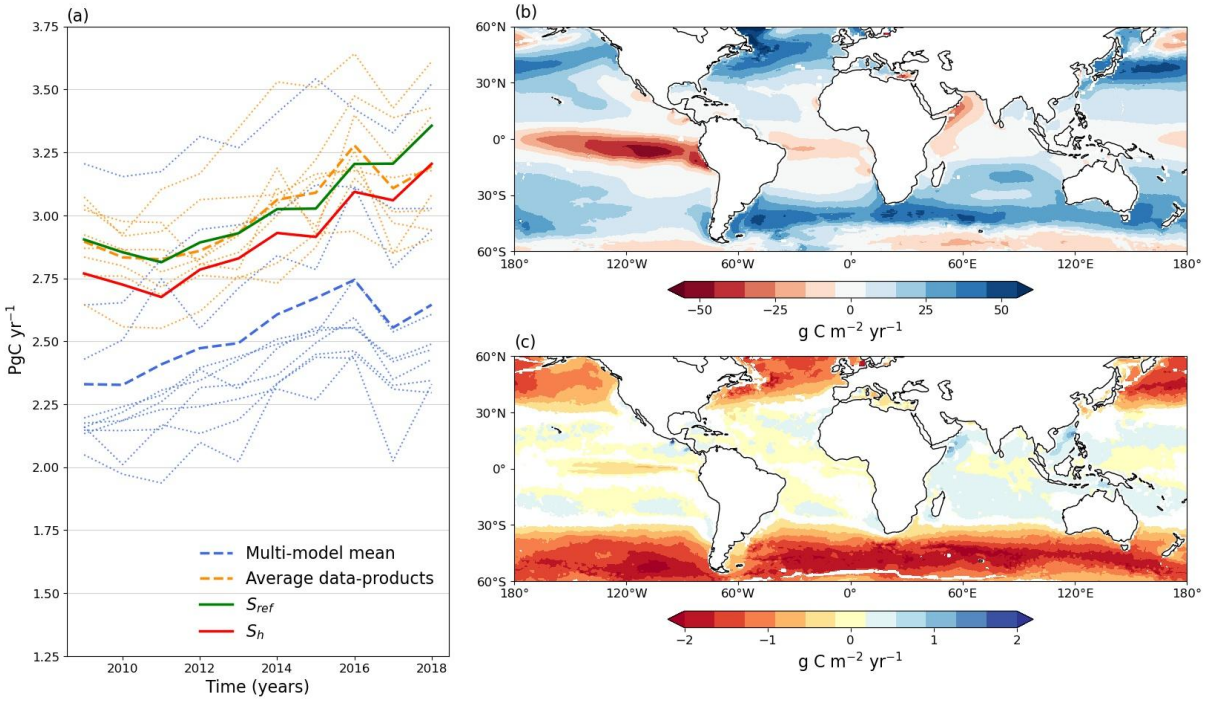

Figure 1. a) Time series of the global (60°N-60°S) annual mean CO_2 sink (Pg C yr $^{-1}$) computed from S_{ref} (thick green line), S_h (thick red line), and the global annual mean from the GCB 2024 data products (thin orange lines) and their mean (thick dashed orange line) as well as the GCB 2024 models (thin blue lines) and their mean (thick dashed blue line). Also shown are maps for the 2009-2018 mean of b) the air-sea CO_2 reference flux F_{ref} and c) the difference between the monthly mean of the high frequency flux $\overline{F_h}$ and F_{ref} , where positive values indicate less outgassing or more uptake with $\overline{F_h}$ than with F_{ref}.

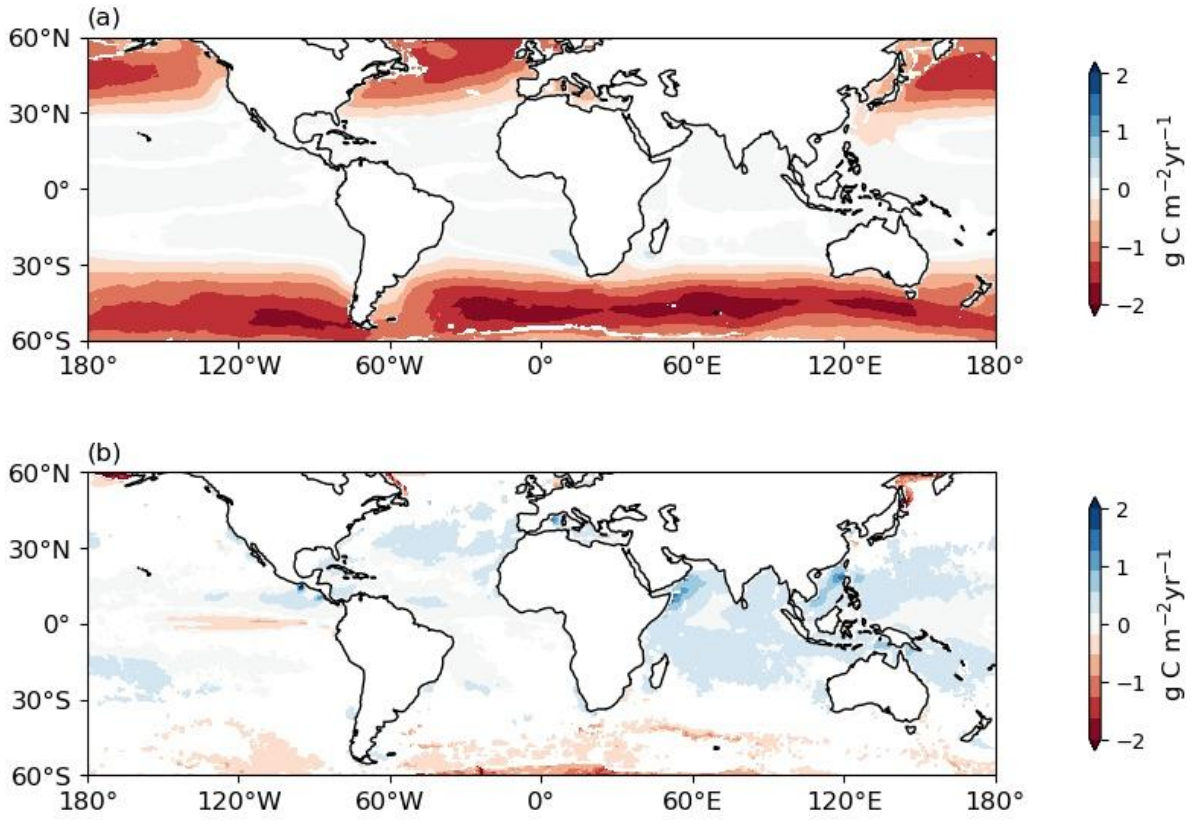

596

597 **Figure 2. Maps averaged over 2009-2018 for effects on observation-based air-sea CO_2**

598 **fluxes from a) submonthly variability of atmospheric pressure ($\overline{F_P} - F_{ref}$) and b)**

599 **submonthly variability of temperature ($\overline{F_{P,T}} - \overline{F_P}$).**

600

601

602

603

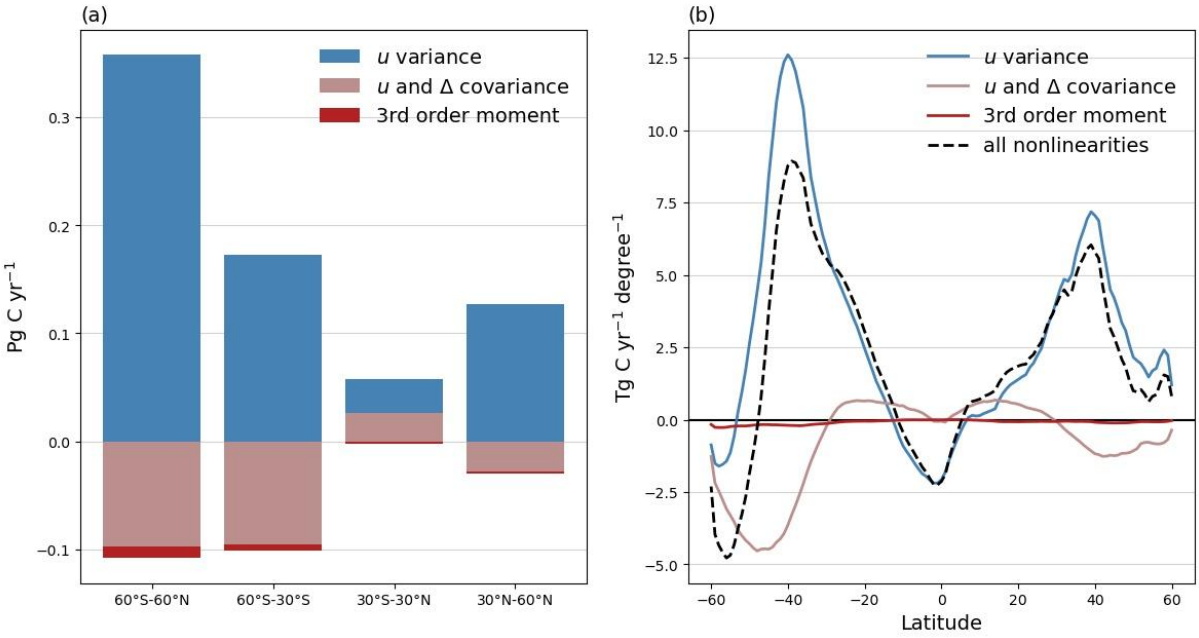

604

605 **Figure 3. a) Contribution of the final 3 terms in equation 5 to ocean carbon uptake in**
606 **different latitudinal bands. b) Zonal integral of the final three terms in equation 5 (blue,**
607 **pink and red lines) and their sum (dashed black line).**